International Journal of Heat and Mass Transfer 52 (2009) 4108–4116

Contents lists available at ScienceDirect

International Journal of Heat and Mass Transfer

journal homepage: www.elsevier.com/locate/ijhmt

Feasibility and optimization of the hollow optical fiber drawing process

Jing Yang *, Yogesh Jaluria

Department of Mechanical and Aerospace Engineering, Rutgers University, Piscataway, NJ 08854, USA

ARTICLE INFO

Article history:
Received 19 November 2008
Accepted 23 March 2009
Available online 15 May 2009

Keywords:
Hollow fiber
Optical fiber
Feasibility
Optimization
Fiber drawing

ABSTRACT

The drawing process for the fabrication of a hollow optical fiber involves the flow of glass, which is largely heated by thermal radiation, in an inert gas environment. It is critical to maintain the central core, which can collapse if the thermal conditions are not properly imposed and controlled. This paper presents the analysis and simulation of this complicated process. A numerical model is developed, validated, and applied to simulate the hollow optical fiber drawing process under a wide range of boundary conditions, particularly draw speed, tension, and temperature. A feasible domain of the drawing process is identified to give the range of the drawing parameters for which the geometry of the fiber is maintained and collapse of the core and viscous rupture of the fiber are avoided. The effects of drawing temperature and feeding speed, which are crucial factors in determining the geometry and quality of the fiber, are investigated in detail. A multi-variable unconstrained optimal design problem is posed and considered in terms of the feasible domain. An appropriate objective function, comprised of the maximum velocity lag, thermally induced defect concentration and draw tension, is proposed to quantify the quality of the hollow fiber. The univariate search method is then applied to obtain the optimal drawing temperature and feeding speed. This study provides a basis for the optimization of hollow fiber drawing process and indicates that a substantial improvement in fiber quality can be achieved.

1. Introduction

Hollow optical fibers have a wide range of applications, from sensors to power delivery and medical applications. A high quality hollow optical fiber is desirable in order to achieve low signal loss. Hollow optical fibers are typically fabricated by drawing a specially manufactured hollow glass preform to the desired fiber diameter in a conventional fiber-drawing tower. The quality of the final hollow fiber can be characterized by many factors, such as draw tension, which can cause stresses and microcracks in the fiber, radial non-uniformity in temperature and velocity, and concentration of drawing-induced defects. Small values of these factors are desirable for high fiber quality. All of these factors strongly depend on the drawing conditions, such as the furnace temperature, the drawing speed, and the preform feeding speed. Therefore, optimizing the hollow fiber drawing system can significantly improve the quality of hollow optical fiber.

A number of studies have been carried out on the solid-core fiber drawing process. Among these, only a few considered the optimal design of the fiber drawing system. For instance, Cheng and Jaluria [1] developed an optimization algorithm. In addition, compared with solid-core fiber drawing, very few researchers [2–5] have investigated the simulation of the hollow optical fiber drawing process. No investigations have been directed at the optimization of the hollow optical fiber drawing process or of the relevant system. However, optimization in hollow optical fiber drawing is strongly needed due to the interest in high quality fiber at high draw speeds. Compared to experimental work, numerical simulation provides a convenient and practical way for optimization because of the cost and effort involved with the former.

This paper presents the optimal design of the hollow optical fiber drawing process, considering the feasible domain of the process. The numerical model of the hollow optical fiber drawing process, presented by Yang and Jaluria [6], is used for optimization. As shown in the earlier study, on the one hand, the central hole in the hollow fiber may collapse completely at high furnace temperatures or at low drawing speeds. On the other hand, lower furnace temperatures or high drawing speeds may cause failure in the drawing process due to viscous rupture, which causes the fiber to break. Hence, the feasible domain for hollow fiber drawing, in which a successful fiber drawing is obtained, must be identified before the drawing system can be optimized to get high quality hollow fibers. Among the main drawing parameters, the furnace temperature and the preform feeding speed significantly affect the drawing process and can be easily and realistically controlled. So the temperature of the drawing furnace and the preform feeding speed are chosen for detailed investigation and optimization of the hollow optical fiber drawing process. The effects on draw tension, maximum temperature and velocity lags, and drawing-induced

* Corresponding author.
E-mail address: jaluria@jove.rutgers.edu (J. Yang).

0017-9310/$ - see front matter © 2009 Elsevier Ltd. All rights reserved.
doi:10.1016/j.ijheatmasstransfer.2009.03.033

Nomenclature

C_r	collapse ratio in hollow fiber drawing
c_p	specific heat at constant pressure
g	acceleration due to gravity
H	height
K	thermal conductivity
L	preform length
n	refractive index
$\vec{n}$	unit normal vector
p	pressure
$\vec{q}$	heat flux
r	radial coordinate distance
R	radius
S_r	radiation source term
t	time
T	temperature
u	radial velocity
v	axial velocity
z	axial coordinate distance
λ	absorbing wavelength band
μ	dynamic viscosity
ν	kinematic viscosity
Φ	viscous dissipation term
ρ	density
τ	shear stress

Subscripts

f	fiber
F	furnace
in	inlet

Superscripts

(1)	core
(2)	cladding

defect centers are investigated. Based on these results, an appropriate objective function for optimization is formulated and a multivariable and non-constrained optimal design problem is presented. Finally, a simple optimization procedure is carried out to solve the problem.

2. Mathematical and numerical modeling

A conjugate problem, involving conduction, convection, and radiation heat transfer mechanisms in hollow optical fiber drawing process, is considered. The mathematical model and the numerical scheme have been presented in the earlier papers. For more details, see Yang and Jaluria [6,7]. Fig. 1 illustrates the geometry and coordinate system for the cylindrical drawing furnace. Only half of the axisymmetric domain is shown for convenience. The flows of glass, and of the internal and external gases in the cylindrical furnace are all taken as laminar, incompressible, and axisymmetric. The buoyancy effects are neglected here on the basis of results obtained earlier [6]. The full governing equations for the gases and the glass are given as:

$$\frac{\partial v}{\partial z}+\frac{1}{r}\frac{\partial (ru)}{\partial r}=0 \tag{1}$$

$$\rho\left(\frac{\partial v}{\partial t}+u\frac{\partial v}{\partial r}+v\frac{\partial v}{\partial z}\right)=-\frac{\partial p}{\partial z}+\left(\frac{1}{r}\frac{\partial}{\partial r}\left(\mu\left(\frac{\partial v}{\partial r}+\frac{\partial u}{\partial z}\right)\right)\right)+2\frac{\partial}{\partial z}\left(\mu\frac{\partial v}{\partial z}\right) \tag{2}$$

$$\rho\left(\frac{\partial u}{\partial t}+u\frac{\partial u}{\partial r}+v\frac{\partial u}{\partial z}\right)=-\frac{\partial p}{\partial r}+\left(\frac{2}{r}\frac{\partial}{\partial r}\left(\mu r\frac{\partial u}{\partial r}\right)\right)+\frac{\partial}{\partial z}\left(\mu\left(\frac{\partial v}{\partial r}+\frac{\partial u}{\partial z}\right)\right) \tag{3}$$

$$\rho C_p\left(\frac{\partial T}{\partial t}+u\frac{\partial T}{\partial r}+v\frac{\partial T}{\partial z}\right)=\frac{1}{r}\frac{\partial}{\partial r}\left(rK\frac{\partial T}{\partial r}\right)+\frac{\partial}{\partial z}\left(K\frac{\partial T}{\partial z}\right)+\Phi+S_r \tag{4}$$

where Φ is the viscous dissipation term and S_r is the radiation source term, which is obtained from radiation analysis within the glass and the furnace. The viscous dissipation term Φ is retained only for the glass flow due to the high viscosity of glass, typically being of the order of a few million times that of water at room temperature

$$\Phi=\mu\left(2\left[\left(\frac{\partial u}{\partial r}\right)^2+\left(\frac{u}{r}\right)^2+\left(\frac{\partial v}{\partial z}\right)^2\right]+\left(\frac{\partial v}{\partial r}+\frac{\partial u}{\partial z}\right)^2\right) \tag{5}$$

For the boundary conditions, at the top of the preform, uniform velocity and temperature are assumed. At the fiber exit, axial diffusion is neglected in the energy and momentum transport. The temperature distribution is specified at the furnace wall, using typical data available on such optical fiber draw furnaces. Along the axis of the furnace and perform/fiber, symmetry is employed. Along the free surfaces ($r = R_1$ and $r = R_2$), the streamfunction values are set equal to constant values and continuity of velocity, temperature and heat flux is applied. The two neck-down profiles are computed on the basis of the balance of the surface forces and mass conservation [6,7].

The vorticity–streamfunction approach is used for solving this problem. The zonal method [8] is applied to model the radiative transport within the glass. The two-band model presented by Myers [9] and adapted by Chen and Jaluria [8] for the absorption coefficient of pure silica is used here. The glass properties are functions of the temperature and are taken from Fleming [10]. The properties of the gas, taken as air, are computed using the state equation of an ideal gas and power law correlations [11], which are expressed as follows:

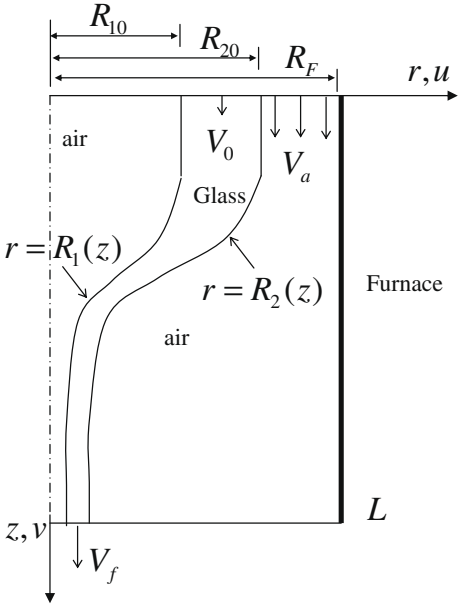

Fig. 1. Schematic diagram of hollow fiber drawing in a furnace.

$$\frac{\rho}{\rho_{ref}} = \frac{T_{ref}}{T}$$
$$\frac{c_p}{(c_p)_{ref}} = \left(\frac{T}{T_{ref}}\right)^{0.104}$$
$$\frac{\mu}{\mu_{ref}} = \left(\frac{T}{T_{ref}}\right)^{0.65} \quad (6)$$
$$\frac{K}{K_{ref}} = \left(\frac{T}{T_{ref}}\right)^{0.79}$$

In the hollow optical fiber drawing process, the geometry may change in terms of the relative dimensions [6]. Thus, a change may occur from the initial preform radius ratio, which is the ratio of the radius R_1 of the hole to the outer radius R_2, resulting in this ratio R_1/R_2 varying downstream. A collapse ratio C_r is defined to describe the collapse process, as:

$$C_r = 1 - \frac{R_1(z)/R_2(z)}{R_{10}/R_{20}} \quad (7)$$

Thus, $C_r = 0$ when the radius ratio of the final fiber equals the initial radius ratio, and $C = 1$ when the central cavity is closed. A complete collapse of the hole would make the process unacceptable or infeasible.

Two different grid schemes are used in the model. The non-uniform grid scheme developed by Lee and Jaluria [12] is applied to solve the governing transport equations. A 369×41 grid is used in the central cavity, a 369×21 grid in the fiber and 369×61 grid in the external gas. A 30×5 coarser grid is used for radiation source term in glass layer. Further grid refinement showed that the results were not significantly affected. The governing transport equations are solved using a false transient scheme, as described in the literature [13]. The equations are discretized using second-order central differencing. The streamfunction, vorticity, and energy equations are solved using an alternating direction implicit (ADI) approach by alternating traverses in the z and r directions, respectively. For any given neck-down profiles, the above false transient iterative procedure is carried out for about 2000 steps to save the computational time, which has been found adequate for the radius correction [14]. Then the neck-down profiles are modified by the numerical corrective procedure. Further details on the computational procedure may be obtained from the references given here, particularly Refs. [6,8]. The mathematical and numerical model has been extensively validated, both for solid core and hollow optical fiber drawing, as presented in these references and is not repeated here.

Draw tension, which can be practically controlled during the drawing process, plays an important role in determining the characteristics and geometry of the final hollow fiber. Draw tension can be obtained by considering all the forces acting at a horizontal cross-section of the preform/fiber. By neglecting the shear force due to internal and external flows, the draw tension F_T for hollow fiber drawing can be expressed as a contribution of viscous, surface tension, gravity, and inertia forces [7]:

$$\begin{aligned} F_T &= F_\mu + F_\zeta + F_I - F_g \\ &= 3\pi\mu\left(R_2^2 - R_1^2\right)\frac{\partial v}{\partial z} + 2\pi\left(\zeta R_2^2 H_2 + \zeta R_1^2 H_1\right) \\ &\quad + \pi\rho\int_z^L \left(R_2^2 - R_1^2\right) v\frac{\partial v}{\partial z}dz - \pi\rho g\int_z^L \left(R_2^2 - R_1^2\right)dz \end{aligned} \quad (8)$$

where F_μ is the force due to glass viscous stress, F_ζ is the force due to surface tension over the two free surfaces, F_I is the force due to inertia, and F_g is the force due to gravity. The draw tension strongly affects the optical and mechanical properties of the fiber in terms of index of refraction, residual stresses, and transmission losses, ultimately influencing the fiber strength and optical quality. A draw tension kept under a specified threshold is critical to achieving continuous pulling of optical fibers without breakage.

It is known that low radial non-uniformity in temperature and velocity in the preform are crucial to the fiber quality because they can cause the redistribution of the material dopants and impurities [15–17]. The relative radial temperature difference between the outer surface and the inner surface, namely the temperature lag, is defined in dimensionless terms as:

$$T_{lag}(z) = \frac{T(r = R_2, z) - T(r = R_1, z)}{T(r = R_2, z)} \quad (9)$$

The temperature lag describes the thermal response in the glass.

Similarly, the dimensionless velocity lag in hollow fiber drawing is expressed as:

$$V_{lag}(z) = \frac{V(r = R_2, z) - V(r = R_1, z)}{V(r = R_2, z)} \quad (10)$$

Lower temperature and velocity lags in the hollow optical fiber drawing process indicate greater uniformity in the radial direction. Therefore, small values of the maximum temperature and velocity lags during the draw process are desired to obtain high quality of the fiber.

The drawing process can generate defects due to the shear and temperatures to which the material is subjected. These drawing-induced defects, such as E' defects, caused by the breaking of the Silicon–Oxygen bond, and non-bridging oxygen hole centers (NBOHCs), are crucial factors in determining the optical properties of fibers since they can cause optical absorption and greater transmission loss. It has been observed that the 630 nm absorption is related to the NBOHCs concentration in high-OH-content silica glass. In low-OH-content silica glass, the 630 nm absorption is related to the sum of the concentrations of NBOHCs, E' defect centers and peroxy radicals [18]. Therefore, investigations of the drawing-induced defect centers have been of interest in the drawing process. Generally, a low value of the defect concentration is desirable for a higher quality of the fiber. The formation mechanisms of these drawing-induced defect centers depend strongly on the drawing conditions and the type of silica glass.

E' defects in silica glass are generated from the breaking of the Si—O bond of a potential precursor. The generation of E' defect depends on the temperature history of the fiber. The model given by Hanafusa et al. [15] can be used to describe the generation of E' defects in the drawing process

$$v\frac{dn_{E'}}{dz} = n_{p0}\bar{\nu}\exp\left(-\frac{E_p}{kT}\right) - n_{E'}\bar{\nu}\left[\exp\left(-\frac{E_p}{kT}\right) + \exp\left(-\frac{E_d}{kT}\right)\right] \quad (11)$$

where $n_{E'}$ is the concentration of E' defects, and n_{p0} is the concentration of the initial precursors, E_p and E_d are corresponding activation energies, $\bar{\nu}$ is the frequency factor, k is the Boltzmann constant. The values of the constants are given by Hanafusa et al. [15]. In the results, the concentrations of E' defects are normalized by the E' defect concentration at T_{melt} in the equilibrium state, i.e. $5.8285 \times 10^{12}\ \mathrm{g}^{-1}$.

The NBOHC defect is another important kind of defect center in optical fiber. The generation of NBOHCs is affected by the shear stress as well as the temperature history undergone by the fiber. The equation to determine NBOHCs can be expressed as [18]:

$$\frac{dN}{dt} = N_0(\sigma/\sigma_0)^b \exp(-E_c/kT)$$

where N_0, σ_0, b, E_c are constants, and the shear stress σ is defined by

$$\sigma(z) = \frac{F}{A(z)}$$

Here, F is the drawing Force and A is the cross-sectional area of the hollow fiber

$$\sigma_0 = \frac{F}{A(0)}$$

Along a streamline, we can write:

$$V\frac{dN}{dz} = N_0(\sigma/\sigma_0)^b \exp(-E_c/kT)$$

Integrating this equation along the streamline:

$$\frac{N(z) - N(0)}{N_0} = \int_0^z \frac{(\sigma/\sigma_0)^b \exp(-E_c/kT)}{V_z} dz$$

where the values of the constants are given by $E_c = 3.8$ eV = 6.114×10^{-19} J, $b = 0.75$. The initial concentration of NBOHCs is taken as zero. The normalized concentration of NBOHCs is defined as:

$$n_{\mathrm{NBOHCs}} = \frac{N(z)}{N_0} \tag{12}$$

Then the equation for the normalized concentration of NBOHCs is expressed as:

$$n_{\mathrm{NBOHCs}} = \int_0^z \frac{(\sigma/\sigma_0)^b \exp(-E_c/kT)}{V_z} dz \tag{13}$$

Based on Eqs. (11) and (13), E' and NBOHCs defect concentrations in the fiber can be obtained during the drawing process.

3. Results and discussions

A typical drawing furnace with specified dimensions is used. The furnace diameter is 7 cm and its length is 30 cm, corresponding to an actual draw tower available for experiments. The inner and outer diameters of the preform are 2.5 cm and 5 cm, respectively. The velocity of the purge gas at the inlet is taken as 0.1 m/s. Pressurization of the gas in the core is neglected. The furnace temperature is assumed to have a parabolic profile with the maximum in the middle and minimum at the two ends. The maximum temperature is referred to as the drawing temperature. The difference between maximum and minimum temperatures is fixed at 500 K. The temperature of the preform T_0 is taken as 300 K. The fiber feeding and drawing speeds are taken as 10 m/s and 3.75 mm/min, respectively. All these selected values represent typically values employed in the available draw tower and used in practical circumstances.

3.1. Feasible domain

The hollow fiber cannot be drawn at any arbitrary combination of critical drawing parameters, as shown in a previous study [7]. Fig. 2 illustrates the feasible domain obtained in terms of drawing temperature and drawing speed. The drawing speed is in the range of 1–20 m/s. It is seen that the drawing process is possible only in the region between the two dashed lines. The left boundary exists because the continuous drawing process may fail due to the lack of material flow at low furnace temperature or high drawing speeds. This is initially indicated by the divergence of the numerical correction scheme for the profiles. Fig. 3 shows the numerical procedure of an infeasible case due to the lack of material flow. It is seen that the neck-down profiles become fairly flat after 12 iterations. This phenomenon is the same as seen in the solid-core fiber drawing process [19]. The right boundary exists only for hollow optical fiber because high furnace temperature or low drawing speeds may cause the central air core to collapse completely. At the right side of this boundary line, the central air core is closed

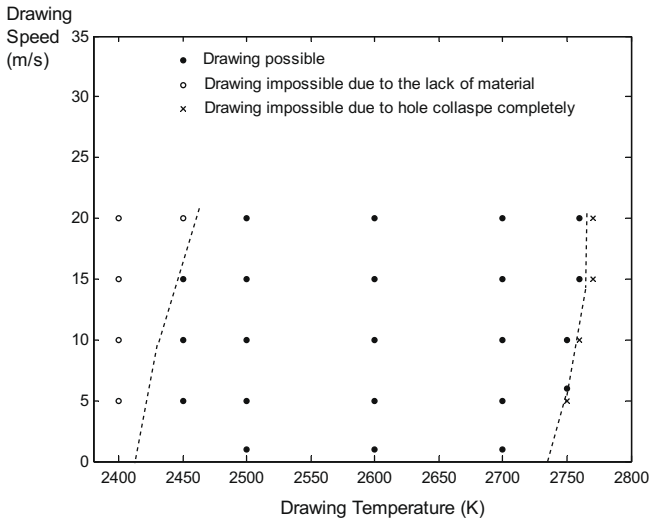

Fig. 2. Feasible domain for hollow fiber drawing in terms of the drawing speed and the drawing temperature.

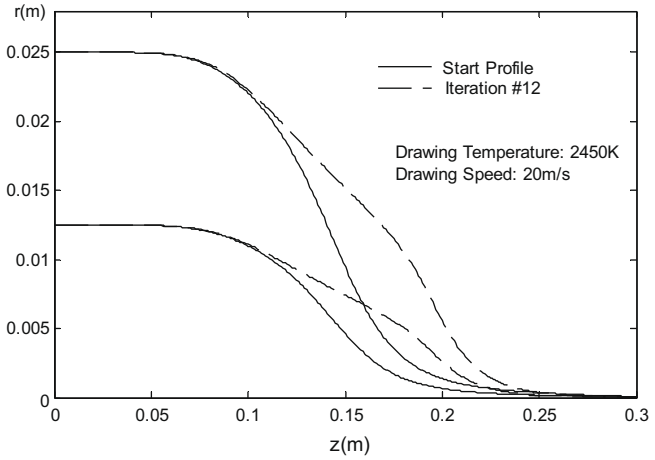

Fig. 3. Neck-down profile corrections for an infeasible drawing case.

during the drawing process. Therefore, there are two thresholds for the drawing temperature at the same drawing speed. These two boundary lines are nearly vertical since the effect of the drawing speed is relatively weak, which has been indicated in an earlier study [6].

3.2. Defects

The generation of the two kinds of drawing-induced defect centers (E' and NBOHCs′) in hollow optical fiber drawing process is investigated. Fig. 4(a) and (b) shows the variations of normalized E' defect and NBOHCs defect concentrations along the axis at different drawing temperatures. The E' and NBOHCs defect concentrations increase along the axis. This trend indicates that E' and NBOHCs defects are generated during the drawing process. It is reasonable because E' and NBOHCs defects are drawing-process-induced defect centers. By comparing Fig. 4(a) and (b), it is seen that the concentration of E' defect increases mainly in the upper neck-down region where the temperature of the fiber increases. But the generation of NBOHCs defects occurs in the whole neck-down region. This is because the generation of E' defect is only dependent on the temperature history of the fiber. In the lower neck-down region the temperature of the fiber reaches the equilibrium temperature. So the concentration of E' defects is also in an

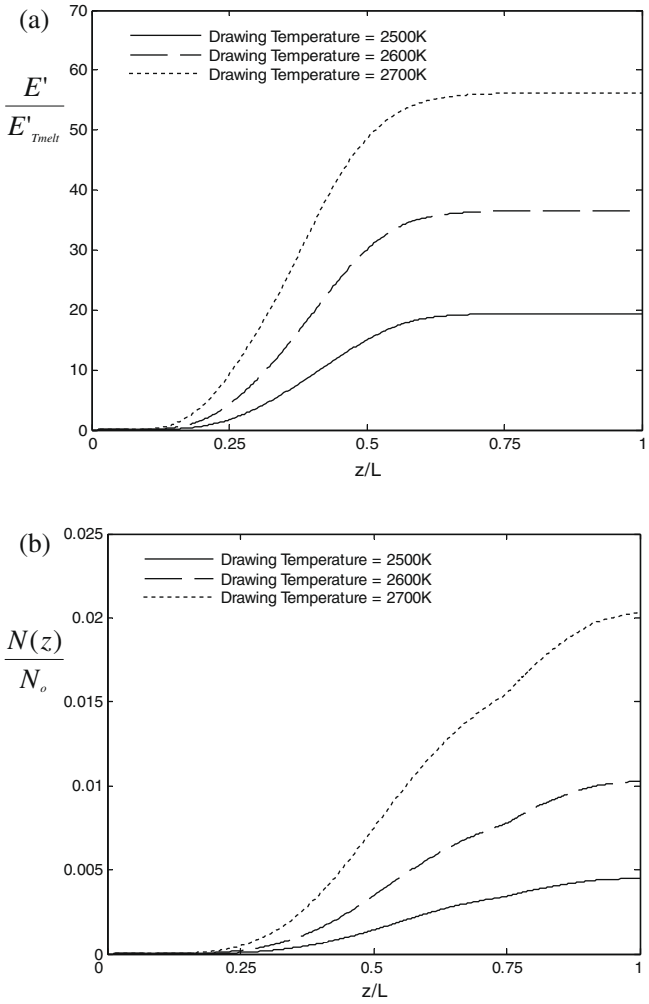

Fig. 4. Variation of normalized concentration of (a) E' defects (b) NBOHCs defects along the axis at different drawing temperatures.

equilibrium state. For NBOHCs defects, the shear stress in the fiber is another important factor besides the temperature history of the fiber. In the lower neck-down region the shear stress increases dramatically due to the decrease of the cross-sectional area of the fiber. This explains why the concentration of NBOHCs defects increases in the entire neck-down region.

The concentrations of E' and NBOHCs defects in the final fibers increase with an increase in the drawing temperature. The reason is that higher drawing temperatures lead to higher temperature of the fiber during the drawing process. The generations of E' and NBOHCs defects are dependent on the temperature of the fiber. Eqs. (11) and (13) indicate that the defect generation terms increase with an increase in the temperature. Therefore, a higher temperature of the fiber leads to higher concentrations of E' and NBOHCs defects.

3.3. Effect of the drawing temperature on the quality of the fiber

The effect of the drawing temperature on the quality of the fiber is investigated. Fig. 5(a) and (b) shows the variation of the maximum velocity and temperature lag at different drawing temperatures. It is seen that the maximum velocity lag is very sensitive to the drawing temperature. But the maximum temperature lag increases only slightly when the drawing temperature increases. These phenomena are similar to those seen for solid-core fiber drawing [19]. The velocity lag has a minimum at a drawing temperature of around 2550 K. The computed levels are more than 0.6 at drawing temperatures of 2450 K and 2750 K. It is high at lower drawing temperatures because the weak heat input at the glass surface results in a slow thermal response in hollow fiber drawing. At higher drawing temperatures, the temperature difference between inner and outer surfaces increases due to thermal inertia. Therefore, the maximum velocity lag is high at large drawing temperatures. The maximum temperature lag is not sensitive to the drawing temperature because it strongly depends on the inlet thermal boundary conditions, which are not changed here.

Fig. 5(c) and (d) shows the concentrations of E' and NBOHCs defect in the final fiber. The concentrations of E' and NBOHCs defects increase by more than 6 times and 10 times in magnitude, respectively, when the drawing temperature goes up from 2450 to 2750 K. Thus, the drawing temperature is the most important factor in generating defects. Higher drawing temperatures enhance the formation of E' and NBOHCs defects due to easier breaking of the Si—O—Si bond at high temperatures. These results suggest that minimizing the drawing temperature can dramatically decrease the E' and NBOHCs defects.

The variation of draw tension with the drawing temperature is shown in Fig. 5(e). The draw tension dramatically increases with a decrease in the drawing temperature. The reason is that the viscous stress increases at lower drawing temperature due to the exponential variation of the glass viscosity with the temperature. Therefore, higher drawing temperatures are desirable in terms of reducing the effect of draw tension on the quality of the hollow fiber. So, clearly, a trade-off is needed since reduced temperatures result in the desired lower defect concentrations and higher temperature in the desired lower tension.

3.4. Effect of feeding speed on fiber quality

The effects of feeding speed are shown in Fig. 6. The feeding speed varies from 3 to 4.5 mm/min. The drawing temperature is 2600 K. It is seen that the feeding speed plays an important role in the E' defect concentration and the draw tension, while the maximum velocity lag, the maximum temperature lag and NBOHC's defect concentration are slightly changed with feeding speed. The draw tension increases with an increase in the feeding speed. These phenomena can be explained in terms of the temperature of the fiber in the drawing furnace. The temperature of the fiber is higher at a lower feeding speed. A higher temperature of the fiber will decrease the viscous force dramatically because glass viscosity decreases exponentially with an increase of temperature. The E' defect concentration decreases with an increase in the feeding speed. It is because a shorter residence time of fiber inside the heating furnace causes less frequent breaking of the Si—O—Si bond.

3.5. Optimization

The univariate search method is used to solve the multivariable optimal design problem considered here. In univariate search method, the multivariable problem is reduced to a series of single-variable optimization problems and then the objective function is optimized with respect to one variable at a time [20,21]. Optimization with respect to the drawing temperature is carried out first. The results discussed before indicates that draw tension, maximum temperature, velocity lag and drawing-induced defect centers, which characterize the quality of the fibers, depend strongly on the drawing temperature of the furnace. Lowering the drawing temperature decreases the drawing defects concentration but increases the draw tension. The velocity lag is large either at high drawing temperature or low drawing temperature. Therefore, an optimum drawing furnace temperature for high quality fiber exists.

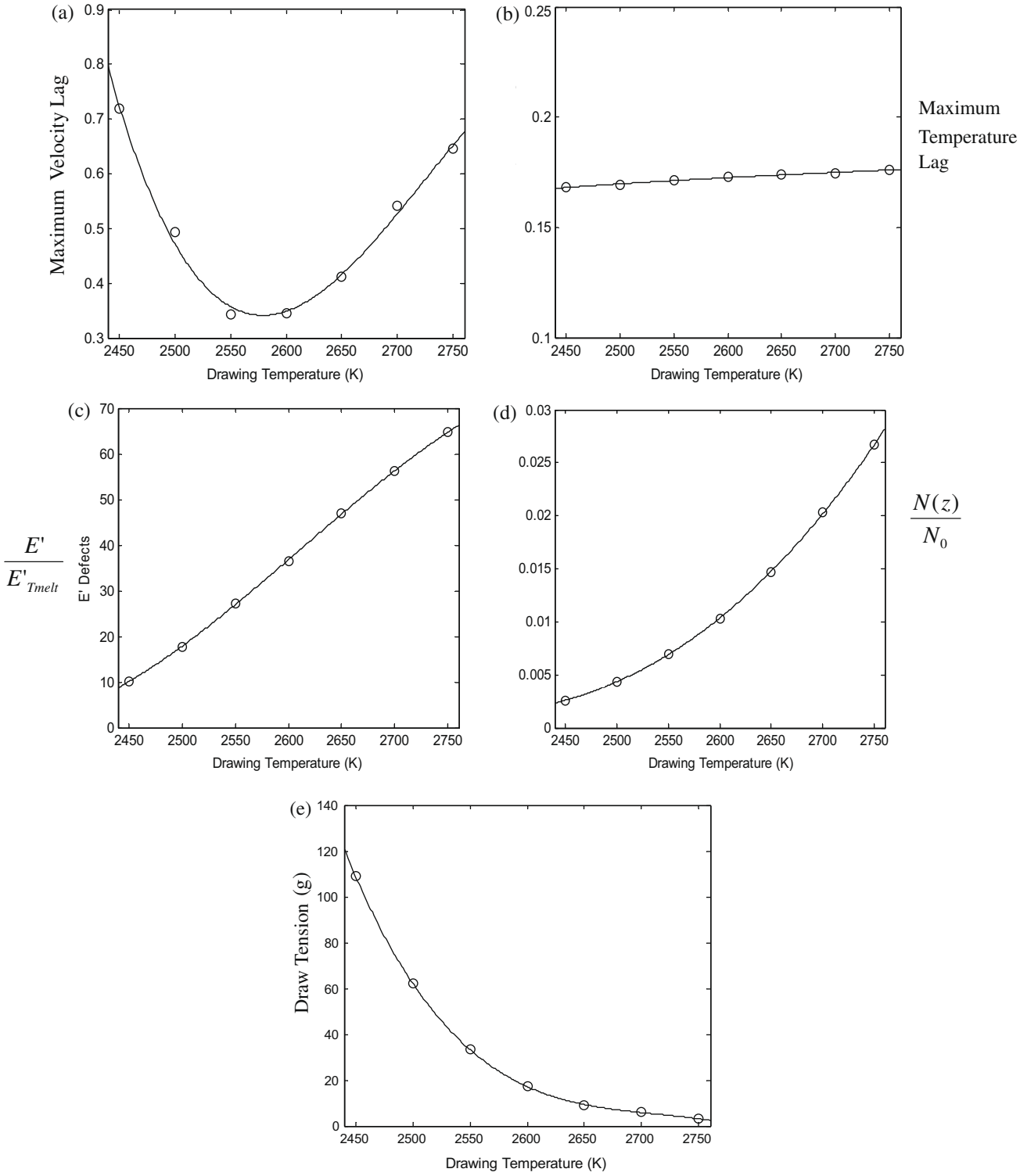

Fig. 5. Variation of (a) maximum temperature lag, (b) maximum velocity lag, (c) E' defect concentration, (d) NBOHC's defect concentration, and (e) draw tension in gram force, with drawing temperature.

The optimization strongly depends on the formulation of the objective function. The drawing conditions for hollow optical fiber drawing can be optimized based on the proper formulation of the application. An objective function in terms of fiber quality is proposed as given below:

$$U = \sqrt{\frac{1}{4}\left(\left(\frac{v_{lag}}{\bar{v}_{lag}}\right)^2 + \left(\frac{n_{E'}}{\bar{n}_{E'}}\right)^2 + \left(\frac{n_{\text{NBOHC's}}}{\bar{n}_{\text{NBOHC's}}}\right)^2 + \left(\frac{F_T}{\bar{F}_T}\right)^2\right)} \tag{14}$$

where four physical quantities, namely the maximum velocity lag, E' and NBOHCs defect concentrations and draw tension, contribute to the quality of the hollow optical fiber. Each variable is normalized by the values at the drawing temperature of 2600 K, which means the objective function equals 1 at a drawing temperature of 2600 K. The reference values for the maximum velocity lag, E' and NBOHCs defect concentration and draw tension are 0.35, 36.55, 0.01, and 17.3 g, respectively. The maximum temperature

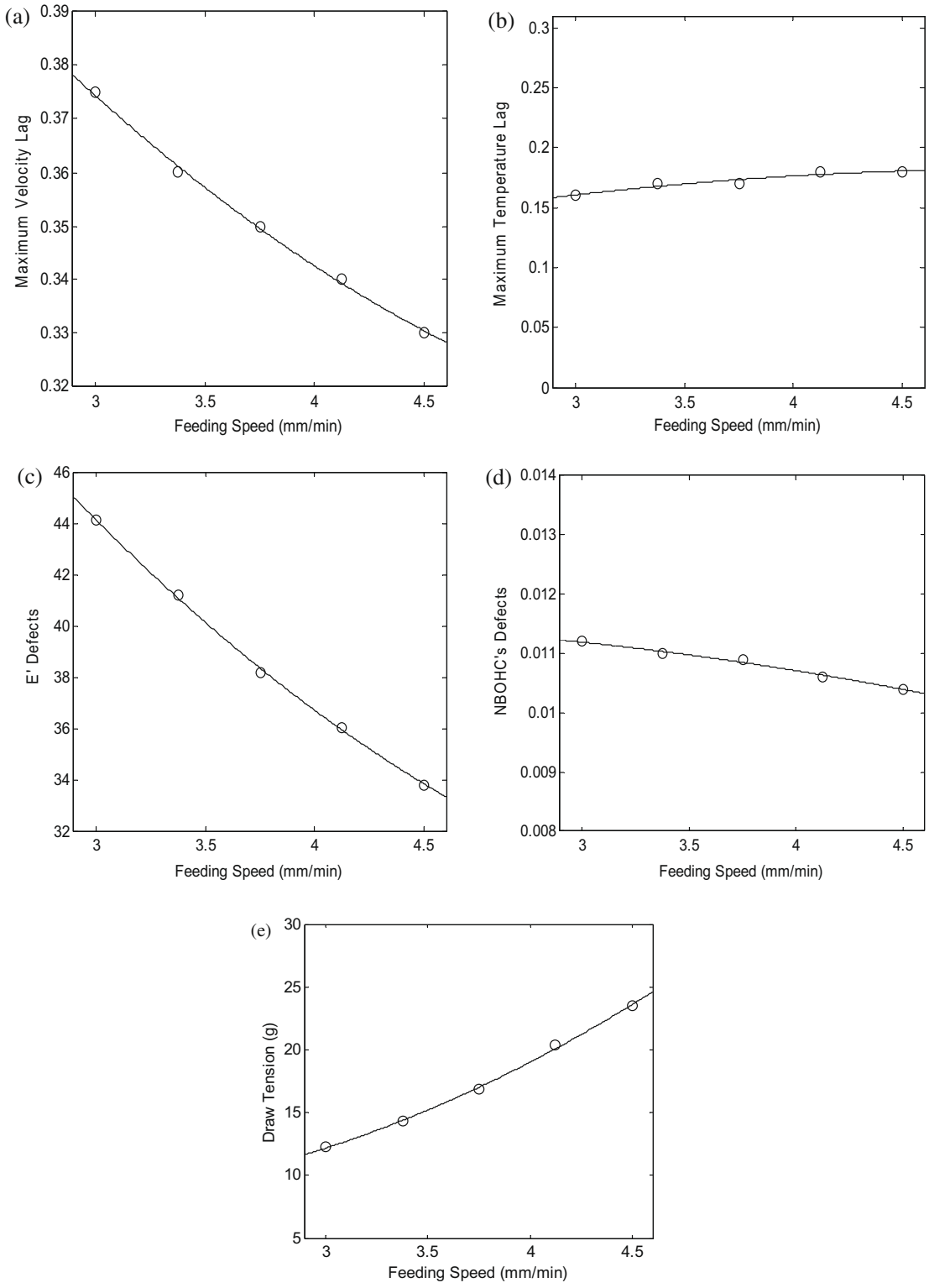

Fig. 6. Variation of (a) maximum temperature lag, (b) maximum velocity lag, (c) normalized E' defect concentration, (d) normalized NBOHC's defect concentration, and (e) Draw tension, with the feeding speed.

lag is eliminated from the objective function due to a sensitivity analysis carried out on the various parameters. At the optimum drawing temperature, the objective function reaches a minimum. The feasible domain for hollow fiber drawing at a drawing speed of 10 m/s gives the following range for the drawing temperature:

$$2450 \leq T \leq 2750$$

All the other drawing parameters except the drawing temperature are fixed at the values mentioned before.

Curve fitting is chosen to solve this single variable and non-constrained optimum problem. A small number of cases are needed for the curve fitting method because the range of the drawing temperature is narrow for hollow optical fiber drawing. Fig. 7 shows the objective function and the curve that represents the results

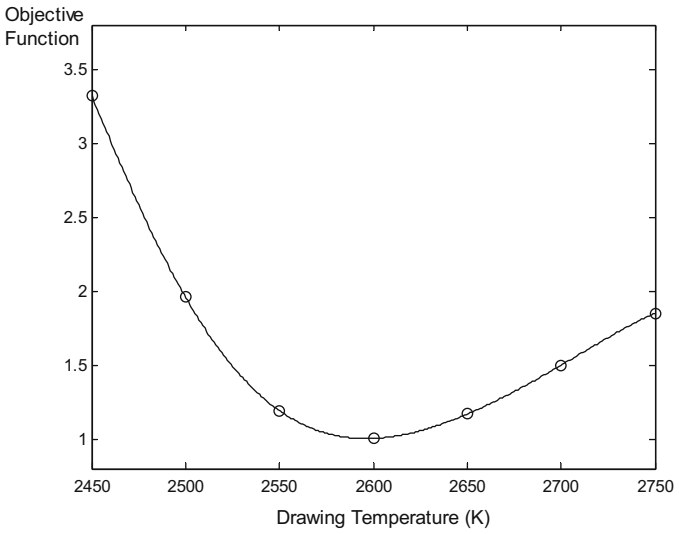

Fig. 7. Variation of the objective function with the drawing temperature using a polynomial curve fit.

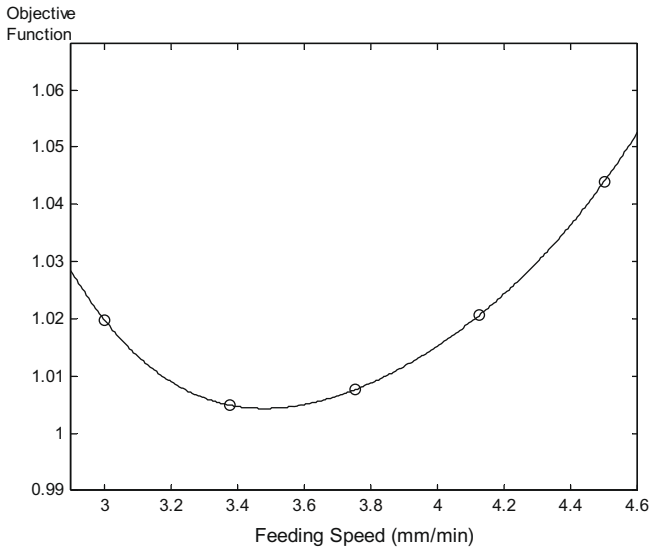

Fig. 8. Variation of the objective function with the feeding speed at a fixed drawing temperature of 2599.1 K and the corresponding polynomial curve fit.

obtained. Here a third, or higher, order polynomial function is applied for curve fitting. It is seen that the objective function decreases sharply and then gradually increases when the drawing temperature increases from 2450 to 2750 K. The minimum of objective function occurs at 2599.1 K where first derivative of the curve fitting function is equal to zero. Therefore, the optimum drawing temperature in the first step is obtained as 2599.1 K. As seen from the variation of the objective function, it may be concluded that the draw tension dominates in hollow fiber quality at lower drawing temperature compared to the effects of defects generation. But at higher drawing temperatures, defect generation contributes more to the objective function than draw tension. Similar trends are also observed in the solid-core fiber drawing process [1]. These can be explained by the exponential variation of the glass viscosity with the drawing temperature.

The results discussed before also indicate that an optimum preform feeding speed for high quality fiber exists. A smaller preform feeding speed can decrease the draw tension. But higher preform feeding speed is desirable to achieve low defect concentration and low velocity lag. Fig. 8 shows the objective function and the curve fit for optimizing the preform feeding speed at a fixed drawing temperature 2599.1 K. The objective function varies almost as a parabola with the preform feeding speed. From this behavior and from the definition of the objective function, we can say that at lower preform feeding speed, the velocity lag, and defect concentration dominate in hollow fiber quality over the draw tension. At higher preform feeding speed, the draw tension contributes more to the objective function. The optimum preform feeding speed, calculated from the polynomial fitting curve, is 3.48 mm/min. By comparing Figs. 7 and 8, it is seen that the value of the objective function is more sensitive to the drawing temperature than to the preform feeding speed over the ranges considered. The objective function varies in the range of $[1, 3.5]$ for the drawing temperature and in the range of $[1, 1.06]$ for the preform feeding speed. Therefore, the drawing temperature plays the dominant role in the optimal design in hollow optical fiber drawing process.

Besides the drawing temperature and the preform feeding speed, the same optimization procedure with the same objective function can be carried out with respect to the other drawing parameters, such as the temperature profile at the furnace wall, the heat zone length, and the diameter of the furnace.

4. Conclusions

A numerical model with a correction scheme for the two neck-down profiles is used for the optimal design of the hollow optical fiber drawing process in this paper. The feasible domain for hollow optical fiber drawing process is presented in terms of the drawing temperature and the drawing speed first. The complete collapse of the central cavity and viscous rupture give the limits for the drawing temperature. The results show that the quality of the fiber, namely maximum velocity lag, drawing-induced defect centers (E' and NBOHCs) and draw tension, strongly depend on the drawing temperature and the preform feeding speed. Either too high or too low value of the drawing temperature or the preform feeding speed will cause low quality of the fiber.

The possibility of optimum design, based on the drawing temperature and the preform feeding speed, is investigated. Then an optimization of the process in terms of the drawing temperature and the preform feeding speed for a typical drawing furnace is carried out. The objective function, comprised of the maximum velocity lag, E' and NBOHCs defect concentrations and draw tension, is defined to characterize the fiber quality. The univariate search method is used to solve the multivariable optimal design problem. The optimum drawing temperature and preform feeding speed are obtained by using curve fitting.

Acknowledgments

The author acknowledges the support of the National Science Foundation, through several grants, and of Corning, Inc., for donated equipment and fiber for much of the work reported here. The author also acknowledges the interactions with Professor C. Polymeropoulos on the optical fiber drawing process.

References

[1] X. Cheng, Y. Jaluria, Optimization of a thermal manufacturing process: drawing of optical fibers, Int. J. Heat Mass Transfer 48 (2005) 3560–3573.
[2] A.D. Fitt, K. Furusawa, T.M. Monro, C.P. Please, Modeling the fabrication of hollow fibers: capillary drawing, J. Lightwave Tech. 19 (12) (2001) 1924–1931.
[3] A.D. Fitt, K. Furusawa, T.M. Monro, C.P. Please, D.J. Richardson, The mathematical modelling of capillary drawing for Holey fibre manufacture, J. Eng. Math. 43 (2002) 201–227.
[4] S.D. Sarboh, S.A. Milinkovic, D.L.J. Debeljkovic, Mathematical model of the glass capillary tube drawing process, Glass Technol. 39 (2) (1998) 53–67.

[5] S.S. Chakravarthy, W.K.S. Chiu, Collapse prediction during hollow optical fiber fabrication, in: 2005 ASME Summer Heat Transfer Conference, San Francisco, California, USA, 2005.
[6] J. Yang, Y. Jaluria, Simulation of hollow optical fiber drawing process, J. Heat Transfer 131 (2009).
[7] J. Yang, Y. Jaluria, Numerical modelling of hollow fiber drawing, in: Proceedings of the 13th International Heat Transfer Conference, Sydney, Australia, Begell House, New York, NY, 2006.
[8] C. Chen, Y. Jaluria, Numerical simulation of transport in optical fiber drawing with core-cladding structure, J. Heat Transfer 129 (2007) 559–567.
[9] M.R. Myers, A model for unsteady analysis of perform drawing, AIChE J. 35 (1989) 592–602.
[10] J.D. Fleming, Fused Silica Manual, Final Report for the U.S. Atomic Energy Commission, Oak Ridge, Tennessee, Project No. B-153, 1964.
[11] D.I. Fotiadis, M. Boekholt, K.F. Jensen, Flow and heat transfer in CVD reactors: comparison of Raman temperature measurements and finite element model predictions, J. Crystal Growth 100 (1990) 577–599.
[12] S.H.-K. Lee, Y. Jaluria, The effects of geometry and temperature variations on the radiative transport during optical fiber drawing, J. Mater. Process. Manufact. Sci. 3 (1995) 317–331.
[13] Y. Jaluria, K.E. Torrance, Computational Heat Transfer, second ed., Taylor & Francis, New York, NY, 2003.
[14] S. Roy Choudhury, Y. Jaluria, S.H.-K. Lee, Generation of the neck-down profile for furnace drawing of optical fiber, Numer. Heat Transfer 35 (1999) 1–24.
[15] H. Hanafusa, Y. Hibino, F. Yamamoto, Formation mechanism of drawing-induced E' centers in silica optical fibers, J. Appl. Phys. 58 (3) (1985) 1356–1361.
[16] Z. Yin, Y. Jaluria, Neckdown and thermally induced defects in high speed optical fiber drawing, ASME J. Heat Transfer 122 (2000) 351–362.
[17] S. Roy Choudhury, Y. Jaluria, Practical aspects in the drawing of an optical fiber, J. Mater. Res. 13 (1998) 483–493.
[18] Y. Hibino, H. Hanafusa, Defect structure and formation mechanism of drawing-induced absorption at 630 nm in silica optical fibers, J. Appl. Phys. 60 (5) (1986) 1797–1801.
[19] X. Cheng, Y. Jaluria, Feasibility of high speed furnace drawing of optical fibers, J. Heat Transfer 126 (2004) 852–857.
[20] C. Chen, Y. Jaluria, Modeling of radiation heat transfer in the drawing of an optical fiber with multi-layer structure, ASME J. Heat Transfer 129 (3) (2007) 342–352.
[21] Y. Jaluria, Design and Optimization of Thermal Systems, McGraw-Hill, 1998.